British Journal of Pharmacology (2008) 153, 34–49
 0007–1188/08 $30.00
www.brjpharmacol.org

RESEARCH PAPER

[Pt(*O,O*′-acac)(γ-acac)(DMS)], a new Pt compound exerting fast cytotoxicity in MCF-7 breast cancer cells via the mitochondrial apoptotic pathway

A Muscella[1], N Calabriso[2], FP Fanizzi[3], SA De Pascali[3], L Urso[2], A Ciccarese[3], D Migoni[3] and S Marsigliante[2]

[1]*General Pathology Laboratory, Dipartimento di Scienze e Tecnologie Biologiche e Ambientali (DiSTeBA), Università di Lecce, Lecce, Italy;* [2]*Cell Physiology Laboratory, Dipartimento di Scienze e Tecnologie Biologiche e Ambientali (DiSTeBA), Università di Lecce, Lecce, Italy and* [3]*General and Inorganic Chemistry Laboratory, Dipartimento di Scienze e Tecnologie Biologiche e Ambientali (DiSTeBA), Università di Lecce, Lecce, Italy*

Background and purpose: We showed previously that a new Pt complex containing an *O,O*′-chelated acetylacetonate ligand (acac) and a dimethylsulphide in the Pt coordination sphere, [Pt(*O,O*′-acac)(γ-acac)(DMS)], induces apoptosis in HeLa cells. The objective of this study was to investigate the hypothesis that [Pt(*O,O*′-acac)(γ-acac)(DMS)] is also cytotoxic in a MCF-7 breast cancer cell line relatively insensitive to cisplatin, and to gain a more detailed analysis of the cell death pathways.
Experimental approach: Cells were treated with Pt compounds and cytotoxicity tests were performed, together with Western blotting of various proteins involved in apoptosis. The mitochondrial membrane potential was assessed by fluorescence microscopy and spectrofluorometry and the Pt bound to cell fractions was measured by atomic absorption spectrometry.
Key results: In contrast to cisplatin, the cytotoxicity of [Pt(*O,O*′-acac)(γ-acac)(DMS)] correlated with cellular accumulation but not with DNA binding. Also, the Pt content in DNA bases was considerably higher for cisplatin than for [Pt(*O,O*′-acac)(γ-acac)(DMS)], thus excluding DNA as a target of [Pt(*O,O*′-acac)(γ-acac)(DMS)]. [Pt(*O,O*′-acac)(γ-acac)(DMS)] exerted high and fast apoptotic processes in MCF-7 cells since it provoked: (a) mitochondria depolarization; (b) cytochrome *c* accumulation in the cytosol; (c) translocation of Bax and truncated-Bid from cytosol to mitochondria and decreased expression of Bcl-2; (d) cleavage of caspases -7 and -9, and PARP degradation; (e) chromatin condensation and DNA fragmentation.
Conclusions and implications: [Pt(*O,O*′-acac)(γ-acac)(DMS)] is highly cytotoxic for MCF-7 cells, cells relatively resistant to many chemotherapeutic agents, as it activates the mitochondrial apoptotic pathway. Hence, [Pt(*O,O*′-acac)(γ-acac)(DMS)] has the potential to provide us with new opportunities for therapeutic intervention.
British Journal of Pharmacology (2008) **153,** 34–49; doi:10.1038/sj.bjp.0707576; published online 19 November 2007

Keywords: [Pt(*O,O*′-acac)(γ-acac)(DMS)]; cisplatin; breast; MCF-7; mitochondrial apoptotic pathway; caspases; Bid; Bcl-2

Abbreviations: DAPI, 4,6-diammine-2-phenylindol; DMEM, Dulbecco's modification of Eagle's medium; DMS, dimethylsulphide; DMSO, dimethylsulphoxide; ECL, enhanced chemiluminescence; ERK, extracellular signal-regulated kinase; MTT, 3-(4,5-dimethylthiazol-2-yl)-2,5-diphenol tetrazolium bromide; PARP, poly(ADP-ribose) polymerase; PBS, phosphate-buffered saline; SDS, sodium dodecyl sulphate; SRB, sulphorhodamine B

Introduction

Platinum-based cancer chemotherapeutic compounds are effective against a variety of malignancies and are used in combination chemotherapy for the treatment of breast cancer (Isaac *et al*., 2002). However, one of the major limitations in their efficacy is that, after an initial response, many tumours become resistant to them. Possible mechanisms of acquired resistance to cisplatin include decreased platinum accumulation, elevated drug inactivation by metallothionein and glutathione, and enhanced DNA repair activity. Increased expression of antiapoptotic genes and mutations in the intrinsic apoptotic pathway may contribute to the inability of cells to detect DNA damage or to induce apoptosis (reviewed by Cepeda *et al*., 2007).

In addition, cisplatin therapy can lead to a number of side effects such as nephrotoxicity, neurotoxicity and emesis. This toxicity of cisplatin limits the dose that can be given to patients (Cepeda *et al*., 2007).

Correspondence: Professor S Marsigliante, Cell Physiology Laboratory, Tecnologie Biologiche e Ambientali (DiSTeBA), University of Lecce, Via prov.le per Monteroni, Lecce 73100, Italy.
E-mail: santo.marsigliante@unile.it
Received 6 August 2007; revised 4 October 2007; accepted 16 October 2007; published online 19 November 2007

These facts together with the aim to find platinum-based derivatives with higher antitumour activity, in order to overcome resistance of many tumour types, have led many investigators to attempt the synthesis and characterization of new platinum analogues. A feature common to all platinum compounds currently in clinical use is that the exchangeable ligands, for example, the two chlorides in *cis*-(diamminedichloro)platinum(II) (cisplatin), are in the *cis* configuration. This requirement is generally regarded as being attributable to the ability of the *cis* compounds to form highly toxic bifunctional intrastrand crosslinks between the N7 atoms of adjacent guanines in double-stranded DNA (Cepeda *et al*., 2007).

In this context, recently, new platinum(II) complexes containing acetylacetonate (acac) in the coordination sphere of the metal have been synthesized: [PtCl(*O,O*′-acac)(DMSO)] with only one oxygen-bonded (*O,O*′-acac) acac, [Pt(*O,O*′-acac)(γ-acac)(DMSO)] containing both an *O,O*′-acac and a σ-bonded (γ-carbon-bonded) acac (De Pascali *et al*., 2005), their dimethylsulphide (DMS) analogues having the same key structures. The ability of these new platinum(II) compounds to induce cell death in human cervical carcinoma HeLa cells has been characterized and compared to the well-established anticancer drug, cisplatin; among them, [Pt(*O,O*′-acac)(γ-acac)(DMS)] exhibited the highest *in vitro* activity from the panel of platinum(II) complexes evaluated (Muscella *et al*., 2007). In addition, the reactivity of the novel complexes with nucleobases and sulphur ligands suggests that the mechanisms that underlie their cytotoxic activity may not necessarily require reaction with DNA (Muscella *et al*., 2007). It is important to note that in mammary epithelium (Xu *et al*., 1995) and in breast cancer cells (Smith, 1999) wild-type p53 protects cells from DNA damage, and generally is not associated with apoptosis (Smith, 1999).

MCF-7 human breast cancer cells are relatively resistant to many chemotherapeutic agents, cisplatin included (Janicke *et al*., 1998; Blanc *et al*., 2000). Since MCF-7 cells do not express full-length caspase-3, because of a 47-bp deletion within exon 3 of the caspase-3 gene, this cell line has become a model for investigation of caspase-3-dependent and caspase-3-independent effects. In addition, the effect of antiapoptotic protein Bcl-2, the transcription of which is upregulated in MCF-7 cells via two oestrogen-responsive elements (Perillo *et al*., 2000), may be an additional protective factor.

The aim of the present study was to characterize the cytotoxic effects of the novel platinum(II) complex [Pt(*O,O*′-acac)(γ-acac)(DMS)] in MCF-7 cells. In addition, the mechanism underlying its activity was also investigated and compared to the well-established anticancer drug, cisplatin. We provided evidence that [Pt(*O,O*′-acac)(γ-acac)(DMS)] may be a promising new therapeutic agent for human cancers.

Methods

Physical measurements

^{1}H NMR spectra were recorded on a Bruker Avance DPX 400, using CD_3OD, $CDCl_3$ and D_2O as solvent. Chemical shifts in CD_3OD and $CDCl_3$ were referred to tetramethylsilane (TMS) by using the residual protic solvent peaks as internal references; chemical shifts in D_2O were referred to TSP (2,2,3,3-*d*(4)-3-(trimethyl-silyl)propionic acid sodium salt), $\delta(H) = 0$ p.p.m., as an external reference. Microanalyses were performed with Carlo Erba Elemental Analyser Mod. 1106 instrument.

Starting materials

Commercial reagent grade dimethylsulphoxide (DMSO) and DMS were supplied by Aldrich. Complex [PtCl(*O,O*′-acac)(DMSO)] and [Pt(*O,O*′-acac)(γ-acac)(DMSO)] were synthesized according to the previously reported procedure (De Pascali *et al*., 2005).

Synthesis of [Pt(O,O′-acac)(γ-acac)(DMS)]

To a solution of [Pt(*O,O*′-acac)(γ-acac)(DMSO)] (0.1 g, 0.21 mmol) in chloroform (3 ml), an excess of DMS (0.130 g, 2.10 mmol) was added and the reaction was left to stir at room temperature overnight. The resulting pale yellow solution was mixed with pentane (10 ml) and kept at 5 °C overnight. The pale yellow crystals of [Pt(*O,O*′-acac)(γ-acac)(DMS)] that formed were isolated, washed with pentane and dried under vacuum (yield 0.070 g, 73%). Anal.calcd for $C_7H_{13}ClO_2PtS$(455.428): C 31.65; H 4.43. Found: C 31.72; H 4.56. ^{1}H NMR in ($CDCl_3$, 298K): δ 1.90s [3H, CH_3(*O,O*′-acac)], 1.95s [3H, CH_3(*O,O*′-acac)], 2.21s [6H, CH_3(γ-acac)], 2.29s [6H, CH_3(DMS), $^3J_{\text{H-Pt}}$ 48 Hz], 4.88 s [1H, C*H*(γ-acac), $^2J_{\text{H-Pt}}$ 125 Hz], 5.47s [1H, C*H*(*O,O*′-acac)].

Reaction of [Pt(O,O′-acac)(γ-acac)(DMS)] with guanosine, 5′-GMP and L-methionine

A solution containing the platinum complex (ca. 2×10^{-3} mmol) and an excess of guanosine (Guo), 5′-GMP or L-methionine (1.6×10^{-2} mmol) dissolved in D_2O (1 ml) was placed in an NMR tube, and the reaction was monitored by ^{1}H NMR spectroscopy. The reaction with Guo and 5′-GMP was negligible after 24 h, whereas the L-methionine instantly reacted with the starting platinum complex.

Compounds stability

The overall loss of water soluble platinum compound under investigation ([Pt(*O,O*′-acac)(γ-acac)(DMS)]) was measured after 24, 48 and 72 h (evaluated by ^{1}H NMR monitoring) and was always found to be negligible in D_2O, in the solutions used in cell culture (0.1% NaCl, phosphate-buffered saline (PBS)) and in Dulbecco's modified Eagle medium (DMEM) with and without a physiological concentration of albumin (40 g l^{-1}) or 10% fetal bovine serum.

Cell culture

MCF-7, MDA-MB-231, SKBR-3 and HBL-100 cell lines were cultured in DMEM supplemented with 10% fetal bovine serum, penicillin (100 U ml^{-1}) and streptomycin (100 μg ml^{-1}). MCF-10A non-cancerous mammary cells were cultured in DMEM/F12 medium supplemented with 5% horse serum,

penicillin (100 U ml^{-1}), streptomycin (100 μg ml^{-1}), hydrocortisone (0.5 μg ml^{-1}) and cholera toxin (0.1 μg ml^{-1}) to stimulate cAMP formation, insulin (10 μg ml^{-1}) and EGF (0.02 μg ml^{-1}). Cells were grown to 70% confluence and then treated with platinum compounds at various concentrations and for different incubation periods.

Cytotoxicity assay

Cells at 70–80% confluency were treated with trypsin (0.25% trypsin with 1 mM EDTA), washed and resuspended in growth medium; 100 μl of a cell suspension (10^5 cells ml^{-1}) was added to each well of a 96-well plate. After overnight incubation, cells were treated with specific reagents for different incubation periods.

The conversion of MTT (3-(4,5-dimethylthiazol-2-yl)-2,5-diphenol tetrazolium bromide) by cells was used as an indicator of cell number as previously described (Muscella *et al*., 2002). This method measures the reduction of MTT by active mitochondria, which results in a colour change measured at 550 nm wavelength. Experiments were performed to define the linear range of the assay. A good correlation was observed up to 50 000 cells per well (data not shown).

Increasing the concentration of heat-killed cells per well (killed by incubating at 70 °C for 15 min) caused no significant change in the absorbance; thus, this spectrophotometric method was a valid technique for measuring the number of viable cells. All subsequent experiments performed were within the linear range of the assay.

The percentage cell survival was calculated as the absorbance ratio of treated to untreated cells. The data presented are means ± s.d. from eight replicate wells per microtitre plate, repeated four times.

Sulphorhodamine B assay

The sulphorhodamine B (SRB) assay was carried out as previously described (Skehan *et al*., 1990). Briefly, 70 μl 0.4% (w v^{-1}) SRB in 1% acetic acid solution was added to each well and left at room temperature for 20 min. SRB was removed and the plates washed five times with 1% acetic acid before air-drying. Bound SRB was dissolved in 200 μl of 10 mM unbuffered Tris–base solution and plates were left on a plate shaker for at least 10 min. Absorbance was measured in a 96-well plate reader at 492 nm. The test optical density value was defined as the absorbance of each individual well minus the blank value ('blank' is the mean optical density of the background control wells, $n = 8$). The percentage survival was calculated as the absorbance ratio of treated to untreated cells. The data presented are means ± s.d. from eight replicate wells per microtitre plate, repeated four times.

Clonogenic survival assay

Cells were seeded in 100 mm Petri dishes at low density ($\sim 3 \times 10^4$ per dish) and left to adhere for 24 h in a standard medium. Crescent concentrations of [Pt(*O*,*O*′-acac)(γ-acac)(DMS)] or cisplatin were added; after 2 h cells were washed, immediately treated with trypsin, resuspended in single-cell suspension, and plated for the determination of macroscopic colony formation. After 15 days of growth, colonies were fixed with a 3:1 mixture of methanol/acetic acid and stained with crystal violet. Only colonies consisting of more than 50 cells were scored. Two separate experiments were performed using duplicate samples.

Trypan blue dye exclusion assay

The cells were seeded in 60 mm tissue culture dishes (100 000 cells ml^{-1}). After overnight incubation, the cells were treated with the concentrations of cisplatin or [Pt(*O*,*O*′-acac)(γ-acac)(DMS)] that were found to produce an IC_{50} and IC_{90} for 12, 24, 48 and 72 h. Cell viability was estimated using the trypan blue exclusion assay and light microscopy.

Preparation of subcellular fraction

To obtain protein cell extracts, cells were washed twice in ice-cold PBS and harvested in 1 ml of PBS. The samples were centrifuged for 30 s at 10 000 *g*, and cell pellets were resuspended in the following buffer (mM): 20 Tris–HCl, pH 8, containing 420 NaCl, 2 EDTA, 2 Na_3VO_4, 0.2% Nonidet P-40 and 10% glycerol, supplemented with a cocktail of protease inhibitors. After a 10 min incubation on ice, cells were passed several times through a 20 gauge syringe and then centrifuged at 13 000 *g* for 10 min at 4 °C. Other samples were centrifuged (100 000 *g*) for 20 min at 4 °C. The resultant supernatant is referred to as the cytosolic fraction.

Nuclei were pelleted by centrifugation at 2000 *g* for 15 min at 4 °C and resuspended in high-salt buffer (20 mM Tris–HCl, pH 7.9, 420 mM NaCl, 10 mM KCl, 0.1 mM $NaVO_4$, 1 mM EDTA, 1 mM EGTA, 20% glycerol, supplemented with a cocktail of protease inhibitors) and sonicated until no nuclei remained intact. Samples were then centrifuged at 13 000 *g* for 10 min at 4 °C, and the resultant supernatant was used as the nuclear extract.

For the preparation of mitochondrial and cytosolic proteins, cells were treated with trypsin, washed once with ice-cold PBS and gently lysed for 30 s in 80 μl ice-cold lysis buffer (250 mM sucrose, 1 mM EDTA, 0.05% digitonin, 25 mM Tris (pH 6.8), 1 mM dithiothreitol, 1 μg ml^{-1} leupeptin, 1 μg ml^{-1} pepstatin, 1 μg ml^{-1} aprotinin, 1 mM benzamidine and 0.1 mM phenylmethylsulphonyl fluoride). The lysate was centrifuged at 12 000 *g* for 3 min at 4 °C to separate the supernatant (mitochondria-free cytosolic extract) and the pellet (mitochondria-containing fraction). Supernatant (40 μg) and pellet (40 μg) were subjected individually to sodium dodecyl sulphate (SDS)-polyacrylamide gel electrophoresis.

The purity of fractions was tested by immunoblotting with antibodies specific to NucP62 (nuclear protein), β-actin (cytoplasmic protein) or porin (mitochondrial membrane protein).

Proteins in the homogenates and cellular fraction were determined using the Bio-Rad protein assay kit 1. Lyophilized bovine serum albumin was used as a standard.

DNA extraction

After drug incubation, cells were washed with PBS and then lysed in a buffer containing 150 mM Tris–HCl, pH 8.0, 100 mM EDTA and 100 mM NaCl, incubated for 15 min at 4 °C and centrifuged at 18 000 *g* for 15 min. Supernatants were treated for 3 h at 37 °C with 20 μg ml^{-1} of proteinase K and then further incubated for 16 h at 37 °C with 4 μl of RNase A of 100 μg ml^{-1}. Finally, DNA was extracted with a volume of phenol/chloroform/isoamyl alcohol (50:49:1), precipitated with 2.5 volumes of cold ethanol and 0.1 volumes of 3 M sodium acetate, washed with 75% of ethanol, dried and resuspended in 1 ml of water. The DNA content in each sample was measured by ultraviolet spectrophotometry at 260 nm.

Platinum determination

To determine total platinum content, cells were washed twice in 0.9% NaCl solution and then digested in 0.5 ml of 65% nitric acid by incubation at 37 °C for at least 2 days to obtain a clear solution.

To determine platinum content in distinct subcellular fractions, cytosolic, nuclear and DNA extracts were digested in 65% nitric acid solution by incubation at 37 °C for at least 2 days to obtain a clear solution.

Platinum content in the samples was determined by atomic absorption spectrometry on a Varian SpectrAA-880Z spectrometer. The reproducibility of measurements, linearity of calibration curve and low limit of detection demonstrated in preliminary studies proved that this method is sensitive and accurate and therefore suitable for determination of platinum content in cells (Muscella *et al*., 2007). All measurements were performed in triplicate and included three quality controls according to standard operating procedures. The cellular platinum levels were expressed as ng of Pt per mg of protein or as pg of Pt per μg of DNA. The data were obtained from four independent experiments with duplicate cultures.

Apoptosis analysis

For DNA fragmentation assay, genomic DNA from MCF-7 cells was prepared using the Wizard genomic DNA purification kit according to the manufacturer's protocol. DNA was dissolved in Tris–EDTA buffer, and 40 μg of DNA was separated on a 1.2% agarose gel containing 0.1 μg ml^{-1} ethidium bromide and visualized under ultraviolet light and photographed.

For 4,6-diammine-2-phenylindol (DAPI) staining, cells treated with cisplatin or [Pt(*O*,*O*′-acac)(γ-acac)(DMS)] were fixed with 3% formalin and stained with 1 μg ml^{-1} DAPI in PBS for 10 min. Cells were mounted on glass slides, covered and analysed using fluorescence microscopy. For statistical analysis of each experiment, 5–10 fields (magnification × 400) were counted (between 400 and 700 cells in total). The mean ± s.d. was calculated and displayed as a bar graph.

Western blot analysis

Total cell proteins or proteins of the distinct subcellular fractions were dissolved in SDS sample buffer and separated on 10 or 15% SDS gels. Separated proteins were transferred electrophoretically onto polyvinylidene difluoride membrane. Equal protein loading was confirmed by Ponceau S staining. Blots were incubated with specific primary antibodies and the immune complexes were detected using appropriate peroxidase-conjugated secondary antibodies and enhanced chemiluminescent detection reagent ECL. Blots were stripped and used for several sequential incubations with control antibodies. Densitometric analysis was carried out on the western blots using the NIH Image 1.62 software (National Institutes of Health, Bethesda, MD, USA). The pixel intensity for each region was analysed, the background was subtracted and the protein expressions were normalized to the porin or β-actin loading control for each lane.

Uptake of JC-1 by mitochondria in MCF-7 cells

Mitochondrial membrane depolarization was detected by a shift in fluorescence emission of the lipophilic cationic probe 5,5′,6,6′-tetrachloro-1,1′,3,3′-tetraethylbenzimidazolocarbocyanine iodide (JC-1) (Smiley *et al*., 1991). JC-1 is able to enter mitochondria selectively, where it exists as a J-aggregate, emitting at 590 nm (red/yellow) after excitation at 488 nm (Smiley *et al*., 1991). Changes in the mitochondrial membrane potential ($\Delta\Psi_m$) and subsequent depolarization result in dissociation of the aggregate into the monomeric form of the dye, causing a shift in emission to 530 nm (green), which can be detected (Smiley *et al*., 1991).

For fluorescence microscopy, cells were grown on 12-mm square glass cover slips (Bradford Scientific, Epping, NH) and changes in the inner mitochondrial transmembrane potential were determined by incubating untreated and cisplatin- or [Pt(*O*,*O*′-acac)(γ-acac)(DMS)]-treated MCF-7 cells with 10 μg ml^{-1} of JC-1 for 15 min at 37 °C in the dark. JC-1 was dissolved in DMSO, stored and used according to the manufacturer's instruction. At the end of each incubation time, the slides were rapidly washed with PBS, drained to prevent formation of crystal of the buffer salts and air-dried. Once completely dried, the slides were mounted with Histovitrex mounting medium without any additional treatment and submitted to fluorescence analysis. Counts of cells with low $\Delta\Psi_m$ were performed on 20 randomly chosen microscopic fields, using a Nikon PCM 2000 microscope (Nikon, Tokyo, Japan).

Spectroscopic analysis

The uptake of JC-1 and the formation of J-aggregates by MCF-7 cells were monitored also by fluorescent spectrophotometer. Inside the mitochondria, the fluorescence emission shifts from green (monomers of JC-1) to red (aggregates). The shifts were detected fluorimetrically (using excitation (EX) 490 nm and emission (EM) 590 nm for red, and 525 nm for green). Mitochondrial depolarization is indicated by a decrease in the red to green fluorescence ratio. Preliminary experiments demonstrated that under these conditions the dye reached near equilibrium distribution and gave a maximal fluorescence response to a fall in $\Delta\Psi_m$ induced by the mitochondrial uncoupler carbonyl-cyanide-*m*-chloro-phenyl-hydrazone (5 μM).

Statistical analysis

Experimental points represent means ± s.d. of 3–6 replicates. Statistical analysis was carried out using the ANOVA. When indicated, *post hoc* tests (Bonferroni/Dunn) were also performed. A *P*-value less than 0.05 was considered to achieve statistical significance.

Reagents

Glutamine, gentamicin, DMEM, fetal bovine serum and the depolarizing agent carbonylcyanide-*m*-chloro-phenyl-hydrazone were obtained from Sigma Chemical Co. (Milan, Italy). Caspase-7, -9, porin, Bid, Bax, Bcl-2, poly(ADP-ribose) polymerase (PARP) and phospho-specific extracellular signal-regulated kinase (ERK)1 and ERK2 antibodies, goat anti-rabbit IgG conjugated with peroxidase, as well as control antibodies, were obtained from Calbiochem Novabiochem (Schwalbach, Germany). All cell lines were purchased from IST Biotech (Genova, Italy).

Protein assay kit 1 was obtained from Bio-Rad (Milan, Italy), proteinase K and RNase A from Sigma, SpectrAA-880Z spectrometer from Varian Inc. (Vacuum Technologies, San Diego, CA, USA), Wizard genomic DNA purification kit from Promega (Madison, WI, USA), polyvinylidene difluoride membrane and chemiluminescent detection reagent ECL from Amersham International (Piscataway, NJ, USA), glass coverslips from Bradford Scientific (Epping, NH, USA), DMSO from Sigma (St Louis, MO, USA), Histovitrex mounting medium from Carlo Erba (Milan, Italy) and JC-1 Kit from Cell Technology (Mountain View, CA, USA).

Results

Synthesis of [Pt(O,O′-acac)(γ-acac)(DMS)] complex

[Pt(*O*,*O*′-acac)(γ-acac)(DMSO)] containing a chelate acetylacetonate (*O*,*O*′-acac) and one σ-bonded (γ-acac) was readily synthesized using methods previously described (De Pascali *et al*., 2005).

In the presence of DMS, this platinum(II) DMSO complex selectively underwent substitution of the sulphur ligand to give the analogous DMS complex [Pt(*O*,*O*′-acac)(γ-acac)(DMS)] (see Figure 1a).

In the reactions with biological nitrogen ligands, such as purines (Guo, 5′-GMP), [Pt(*O*,*O*′-acac)(γ-acac)(DMSO)] showed little reactivity even after several hours, whereas it gave fast substitution of DMSO in the presence of biological sulphur ligands (L-methionine) (Muscella *et al*., 2007). The same selective reactivity in the substitution of the soft sulphur ligand was observed in the reaction of the water soluble [Pt(*O*,*O*′-acac)(γ-acac)(DMS)] with L-methionine, with respect to Guo and 5′-GMP (Figures 1b and c). This selectivity could be also operating when the substitution at the metal involves biological sulphur ligands such as proteic thiol and/or thioethers.

Cytotoxicity of the drugs

The cytotoxicity data shown here were obtained by MTT metabolic assay and confirmed by SRB assay to rule out potential effects of platinum compounds on mitochondrial enzymes. Indeed, comparable results were obtained when cell number was directly determined by cell counting;

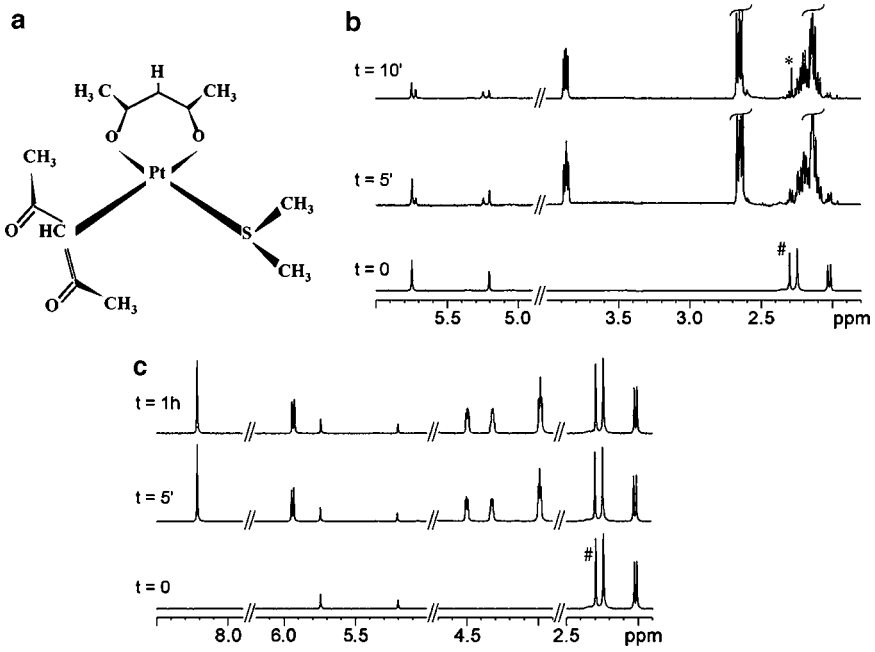

Figure 1 (**a**) Chemical structures of [Pt(*O*,*O*′-acac)(γ-acac)(DMS)] and its reactivity with Guo and L-methionine. ^{1}H NMR spectra in D_2O (400.13 MHz, standard TSP) of [Pt(*O*,*O*′-acac)(γ-acac)(DMS)] with excess of L-methionine (**b**) and 5′-GMP (**c**) at different reaction times. For the complex rapid reaction with methionine, a decrease in the coordinated (#) and increase of free DMS (*) signals, but a negligible reaction with 5′-GMP, was observed. ^{1}H NMR experiments were recorded on a Bruker Avance DPX 400 instrument using D_2O as solvent. ^{1}H NMR chemical shifts were referenced to TSP (2,2,3,3-*d*(4)-3-(trimethyl-silyl)propionic acid sodium salt), $\delta(H) = 0$ p.p.m., in D_2O as an external reference.

consequently, we used the MTT assay in the combined experiments described.

Exposure of the MCF-7 cells to cisplatin and to [Pt(*O*,*O*′-acac)(γ-acac)(DMS)] at concentrations ranging from 1 to 200 μM resulted in a dose-dependent inhibition of cell survival (MTT assay) (Figure 2). [Pt(*O*,*O*′-acac)(γ-acac)(DMS)] showed cytotoxicity approximately 90-fold greater than that observed for cisplatin (for [Pt(*O*,*O*′-acac)(γ-acac)(DMS)], IC_{50} 0.625 ± 0.044 μM; for cisplatin, IC_{50} 56.25 ± 1.5 μM; $n = 4$) (see Figure 2). To determine whether [Pt(*O*,*O*′-acac)(γ-acac)(DMS)] cytotoxicity could be influenced by the expression of oestrogen receptors (ERs), we tested two other breast cancer cell lines, MDA-MB-231 (ERα negative, ERβ positive) (Girdler *et al*., 2001) and SKBR-3 (ERα and ERβ negative) (Filardo *et al*., 2000). Furthermore, we also included two cell lines derived from non-cancerous breast, the simian virus 40-transformed, tumorigenic HBL-100 cell line derived from lactating breast (ER negative) and the MCF-10A non-tumorigenic breast epithelial cells (very low ER) (Hu *et al*., 1998). The IC_{50} values of platinum(II) analogues after 72 h of treatment obtained in all the cell lines are presented in Table 1. [Pt(*O*,*O*′-acac)(γ-acac)(DMS)] was significantly more cytotoxic than cisplatin in all of the cell lines except MCF-10A, where the IC_{50} values obtained were not significantly different ($P > 0.05$).

Clonogenic assay was performed on MCF-7 and MCF-10A cells (Figure 3): [Pt(*O*,*O*′-acac)(γ-acac)(DMS)] was significantly more cytotoxic than cisplatin in MCF-7 cells (Figure 3a). Conversely, in MCF-10A cisplatin was slightly, but significantly, more toxic than [Pt(*O*,*O*′-acac)(γ-acac)(DMS)] only at concentrations in the range 5–25 μM (Figure 3b).

Interestingly, about 50% of cells died after only 3 h of treatment with 100 μM [Pt(*O*,*O*′-acac)(γ-acac)(DMS)], while it was necessary to incubate for about 36 h to get the same effect using 100 μM cisplatin (Figure 4).

IC_{50} and IC_{90} concentrations of [Pt(*O*,*O*′-acac)(γ-acac)(DMS)] and cisplatin caused a time- and dose-dependent decrease in cell number with a parallel increase in the percentage of floating cells (data not shown).

Accumulation of new platinum(II) compound and cisplatin in MCF-7 cells

As previously reported for cisplatin (Gately and Howell, 1993) and for [Pt(*O*,*O*′-acac)(γ-acac)(DMS)] in HeLa cell line (Muscella *et al*., 2007), cellular accumulation measurements showed that [Pt(*O*,*O*′-acac)(γ-acac)(DMS)] accumulated in a linear manner that was correlated with the drug concentration up to the highest concentration tested, 100 μM. This

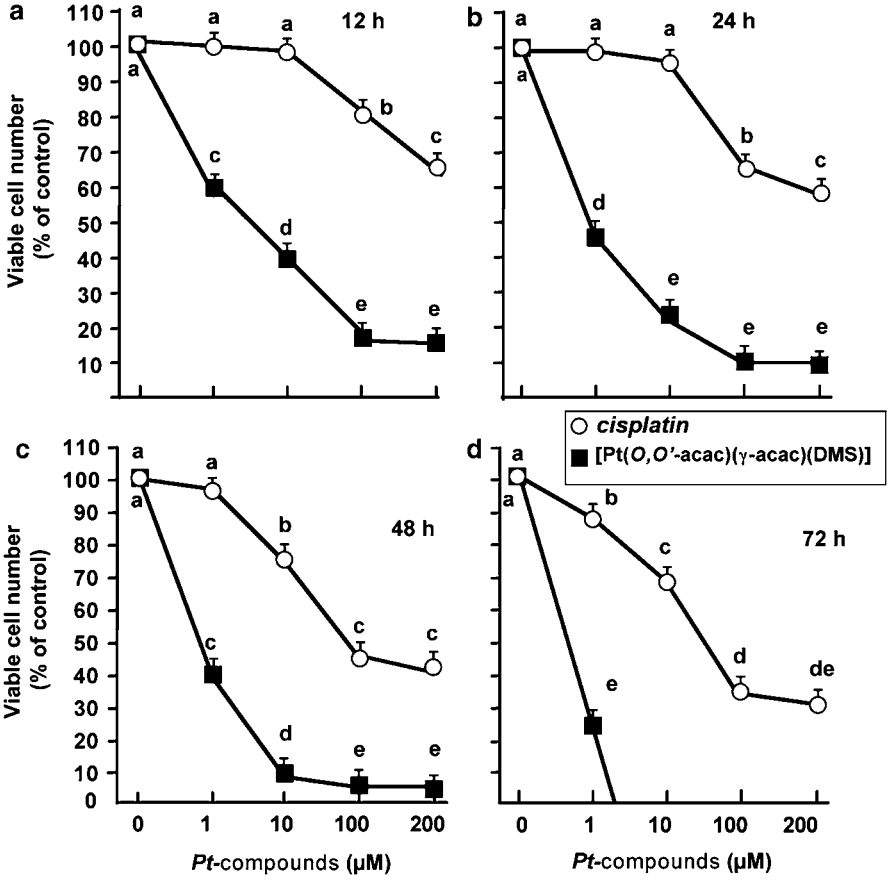

Figure 2 The sensitivity of MCF-7 cells to [Pt(*O*,*O*′-acac)(γ-acac)(DMS)] and cisplatin. Cells were treated with and without increasing concentrations of cisplatin and [Pt(*O*,*O*′-acac)(γ-acac)(DMS)]; viable cell number was determined 12 h (**a**), 24 h (**b**), 48 h (**c**) and 72 h (**d**) later by MTT assay. The data are means ± s.d. of four different experiments, with eight replicates in each, and are presented as % of control. Values with shared letters are not significantly different according to Bonferroni/Dunn *post hoc* tests.

indicates that there is no saturation of the uptake of drugs at concentrations in this range. After treatment with equimolar drug concentrations, the rate of platinum accumulation was higher in [Pt(*O,O*′-acac)(γ-acac)(DMS)] than that in cisplatin. The kinetics of [Pt(*O,O*′-acac)(γ-acac)(DMS)] uptake were different from those of cisplatin; [Pt(*O,O*′-acac)(γ-acac)(DMS)] concentrations in MCF-7 cells increased fast and reached maximum levels after 6 h, when its cellular accumulation was approximately 25-fold higher than that of cisplatin ($P<0.001$) (Figure 4).

After 24 h incubation of MCF-7 cells with 100 μM cisplatin, the total platinum content was 75 ± 10 ng Pt per mg protein; an equivalent platinum cellular content was obtained by using 10 μM [Pt(*O,O*′-acac)(γ-acac)(DMS)]. These concentrations (100 and 10 μM) caused a similar dose-dependent platinum uptake by whole cells for both cisplatin and [Pt(*O,O*′-acac)(γ-acac)(DMS)] (Figures 5a and b). However, the platinum content in DNA bases was considerably higher for cisplatin than for [Pt(*O,O*′-acac)(γ-acac)(DMS)], thus excluding DNA as a target of [Pt(*O,O*′-acac)(γ-acac)(DMS)] (Figures 6a and b). Since the higher cytotoxicity of [Pt(*O,O*′-acac)(γ-acac)(DMS)] could be due to its increased intracellular uptake, concentrations of 100 and 10 μM for cisplatin and [Pt(*O,O*′-acac)(γ-acac)(DMS)], respectively, were also used in subsequent experiments to study and compare the characteristics of apoptosis provoked by these platinum compounds (Figure 6c).

To determine whether the cytotoxicity of [Pt(*O,O*′-acac)(γ-acac)(DMS)] and cisplatin was correlated with the accumulation and/or DNA binding in the MCF-7 cells, the previously obtained data were subjected to linear regression analysis (Figure 6d). We found a significant correlation between cytotoxicity and cellular accumulation of cisplatin ($r^2=0.971$, $P=0.0145$), as well as DNA binding ($r^2=0.998$, $P=0.0248$). However, the cytotoxicity of [Pt(*O,O*′-acac)(γ-acac)(DMS)] correlated only with cellular accumulation ($r^2=0.933$, $P=0.0213$) and not with DNA binding ($r^2=0.52$, $P=0.166$).

Table 1 The IC_{50} values after a 72 h exposure to cisplatin and [Pt(*O,O*′-acac)(γ-acac)(DMS)]

	Cisplatin (μM)	*[Pt(O,O′-acac)(γ-acac)(DMS)] (μM)*
MCF-7	56.25 ± 1.5	0.62 ± 0.04
MDA-MB-231	48.5 ± 3.7	9.7 ± 0.09
SKBR-3	21.3 ± 4.2	5.25 ± 0.3
HBL-100	9.75 ± 0.5	4.75 ± 0.8
MCF-10A	38.53 ± 2.3	40.23 ± 2.2

Abbreviations: acac, acetylacetonate; DMS, dimethylsulphide.

Induction of apoptosis by [Pt(O,O′-acac)(γ-acac)(DMS)]

The results shown in Figure 7a indicate that [Pt(*O,O*′-acac)(γ-acac)(DMS)] induced more DNA fragmentation than cisplatin. Figures 7b–d show the results of a DAPI (known to form fluorescent complexes with natural double-stranded DNA) staining; nuclei are considered to have the normal pheno-

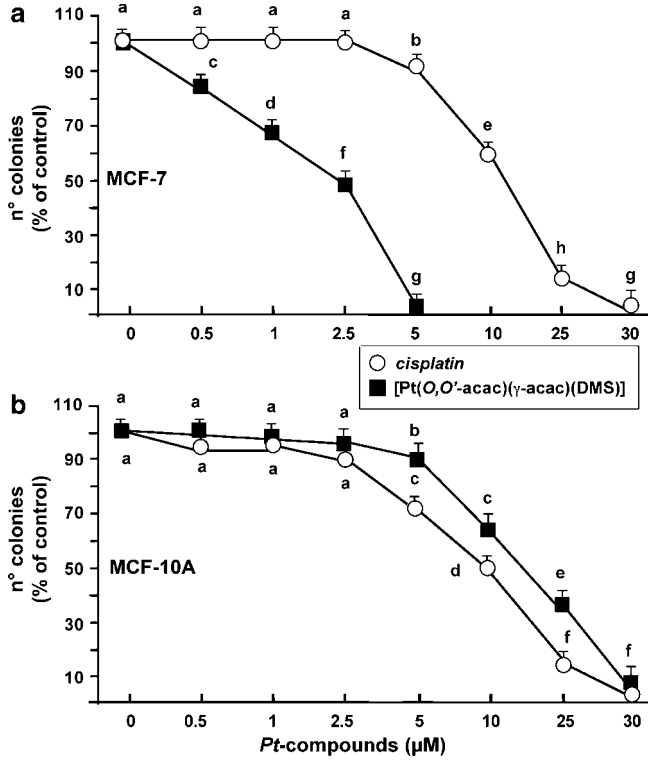

Figure 3 Clonogenic survival assay in cells treated with [Pt(*O,O*′-acac)(γ-acac)(DMS)] and cisplatin. MCF-7 (**a**) and MCF-10A (**b**) cells were exposed to the indicated amounts of cisplatin or [Pt(*O,O*′-acac)(γ-acac)(DMS)] for 2 h, and after 15 days of growth, colonies consisting of more than 50 cells were scored. The percentage survival shown represents the mean ± s.d. of two independent experiments each performed in duplicate. Values with shared letters are not significantly different according to Bonferroni/Dunn *post hoc* tests.

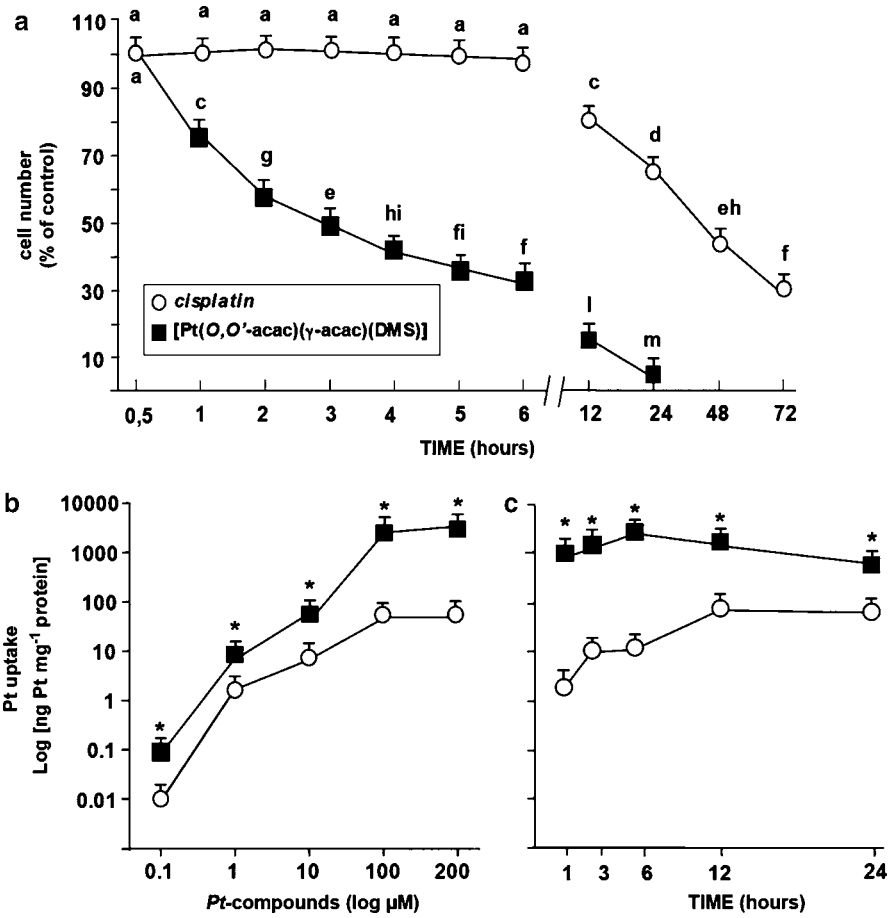

Figure 4 Different dynamics of [Pt(*O,O*′-acac)(γ-acac)(DMS)] and cisplatin effects on MCF-7 cells. (**a**) Cells were continuously exposed to 100 μM of cisplatin or [Pt(*O,O*′-acac)(γ-acac)(DMS)], and cell viability was monitored by MTT assay over a period of 72 h. The data are means ± s.d. of four different experiments each with eight replicates and are presented as % of control. Values with shared letters are not significantly different according to Bonferroni/Dunn *post hoc* tests. (**b**) Cells were exposed to increasing concentrations (0–200 μM) of [Pt(*O,O*′-acac)(γ-acac)(DMS)] and cisplatin for 6 h. (**c**) Cells were exposed to 100 μM of cisplatin or [Pt(*O,O*′-acac)(γ-acac)(DMS)] for the indicated period. Intracellular accumulation was determined by atomic absorption spectrometry. Each point represents the means ± s.d. of three different experiments. Asterisks indicate values that are significantly different ($P<0.05$) from cisplatin at the same concentration and the same time point.

type when glowing bright and homogeneously (Figure 7b). The condensed chromatin gathering at the periphery of the nuclear membrane depicts apoptotic nuclei or a total fragmented morphology of nuclear bodies. Between 400 and 700 cells in 5–10 fields (magnification ×400) were counted and the percentage of apoptotic nuclei determined after varying incubation times. The data obtained are shown in Figure 7e (10 μm of [Pt(*O,O*′-acac)(γ-acac)(DMS)]) and Figure 7f (100 μm of cisplatin). The time course of the nuclear changes revealed that MCF-7 cells reacted differently from platinum compounds inasmuch as 50% of apoptotic cells were seen after 3 h of treatment with [Pt(*O,O*′-acac)(γ-acac)(DMS)] but after 48 h of treatment with cisplatin.

To compare the pathways leading to the induction of cell death in response to DNA damage caused by cisplatin and [Pt(*O,O*′-acac)(γ-acac)(DMS)], the cleavage patterns of caspase-7 and -9, and PARP were analysed by western blotting. PARP, a 113-kDa nuclear protein, has been shown to be one of the first proteins specifically cleaved by caspase-3 and -7 during apoptosis (Kaufmann *et al*., 1993). Therefore, PARP cleavage was examined by western blotting of proteins obtained from isolated nuclei. As shown in Figure 8, both 100 μM cisplatin and 10 μM [Pt(*O,O*′-acac)(γ-acac)(DMS)] significantly increased the amounts of cleaved PARP, thus confirming the early signs of apoptosis process. PARP degradation was already evident after 1 h of [Pt(*O,O*′-acac)(γ-acac)(DMS)] treatment, while cisplatin provoked the fragmentation of PARP (89 kDa fragment) after 9 h of treatment, and this hydrolysis proceeded so slowly that intact PARP was still present after 48 h. Sequential incubation of the blot with anti-actin antibody confirmed that the amount of protein loaded was the same.

Both [Pt(*O,O*′-acac)(γ-acac)(DMS)] and cisplatin caused the proteolysis of procaspase-7; this cleavage occurred faster in the [Pt(*O,O*′-acac)(γ-acac)(DMS)]-treated cells (Figure 8).

Finally, we examined caspase-9, known to be the predominant activator of caspase-7, although some alternative pathways have also been described (Boatright and Salvesen, 2003). We found that the earliest generation of the activated caspase-9 heterodimers, after drug administration, preceded

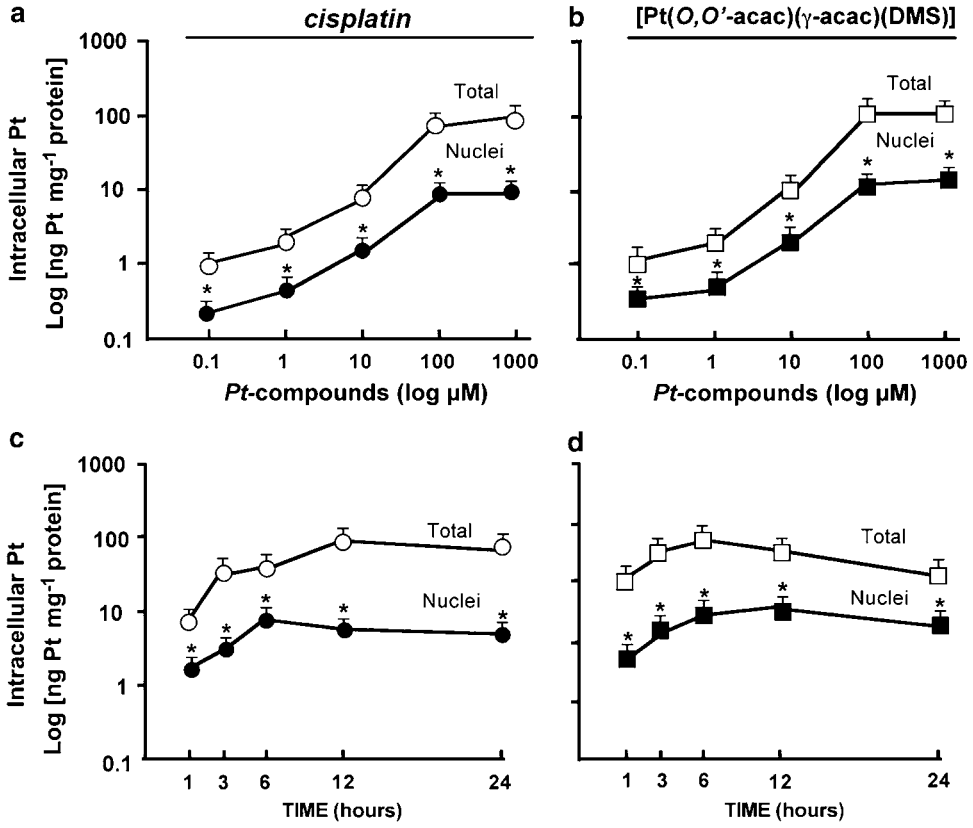

Figure 5 Distribution of platinum in MCF-7 cells. Cells were treated with or without increasing concentration of cisplatin (**a**) or [Pt(*O,O*′-acac)(γ-acac)(DMS)] (**b**). Cells were treated with or without 100 μM cisplatin (**c**) or 10 μM [Pt(*O,O*′-acac)(γ-acac)(DMS)] (**d**) for the indicated period. Total cellular and nuclear platinum in MCF-7 cells treated with cisplatin or [Pt(*O,O*′-acac)(γ-acac)(DMS)] was determined by atomic absorption spectrometry. Each point represents the means ± s.d. of three different experiments. Asterisks indicate values that are significantly different ($P<0.05$) from cisplatin at the same concentration and the same time point.

the activation of caspase-7 in both cisplatin- and [Pt(*O,O*′-acac)(γ-acac)(DMS)]-treated MCF-7 cells (Figure 8).

To determine whether cisplatin and [Pt(*O,O*′-acac)(γ-acac)(DMS)] altered the expression of proteins related to cell death, we assessed the expression of Bid, Bax and Bcl-2 proteins by western blot analysis in whole lysates of MCF-7 treated with 10 μM [Pt(*O,O*′-acac)(γ-acac)(DMS)] or 100 μM cisplatin for various times. Neither cisplatin nor [Pt(*O,O*′-acac)(γ-acac)(DMS)] treatment altered Bax expression; conversely, the expression of Bcl-2 decreased in MCF-7 cells exposed to [Pt(*O,O*′-acac)(γ-acac)(DMS)] and increased in cisplatin-treated cells (Figure 8). The expression of Bid increased markedly in MCF-7 cells exposed to both [Pt(*O,O*′-acac)(γ-acac)(DMS)] and cisplatin. A cleavage of Bid into a truncated protein (t-Bid) (Figure 8), together with its translocation from the cytosol to mitochondria that proceeded the reduction of $\Delta\Psi_m$, was also observed in cells treated with [Pt(*O,O*′-acac)(γ-acac)(DMS)] (Figure 10).

*Effect of cisplatin and [Pt(*O,O′*-acac)(γ-acac)(DMS)] on $\Delta\Psi_m$ in MCF-7 cells*

A reduction in $\Delta\Psi_m$ accompanies early apoptosis in many systems and is believed to be mediated by the opening of the mitochondrial permeability transition pore (PTP), a multi-protein complex (reviewed by Kroemer *et al*., 1998). $\Delta\Psi_m$ was monitored by fluorescence of the cationic lipophilic dye JC-1 in MCF-7 cells treated with a crescent concentration of cisplatin or [Pt(*O,O*′-acac)(γ-acac)(DMS)]. JC-1 possesses the ability to form multimers known as J-aggregates after accumulation in mitochondria with high membrane potential (Smiley *et al*., 1991). In addition to J-aggregates, JC-1 can form monomers in mitochondria with low membrane potential (Smiley *et al*., 1991). Thus, JC-1 can separate two populations of cells by colour code, showing mitochondria with high membrane potential, dyed in red–orange, and low membrane potential, dyed in green. Figure 9a illustrates how these colours may be detected in JC-1-stained MCF-7 cells, known to have high $\Delta\Psi_m$ values (Smiley *et al*., 1991). In cells treated with 10 μM [Pt(*O,O*′-acac)(γ-acac)(DMS)], brilliant red-stained mitochondria progressively decreased and after 3 h only green-stained cells were observed.

Mitochondrial membrane depolarization was also detected fluorimetrically by a shift in fluorescence emission of JC-1; after addition of [Pt(*O,O*′-acac)(γ-acac)(DMS)], $\Delta\Psi_m$ decreased slowly and gradually even after 30 min, as determined by mean aggregate fluorescence of JC-1 (Figure 9c); conversely, $\Delta\Psi_m$ remained high in cisplatin-treated cells for at least 8 h (Figure 9b). Noteworthy, after 100 min of [Pt(*O,O*′-acac)(γ-acac)(DMS)] incubation, $\Delta\Psi_m$ was dissipated

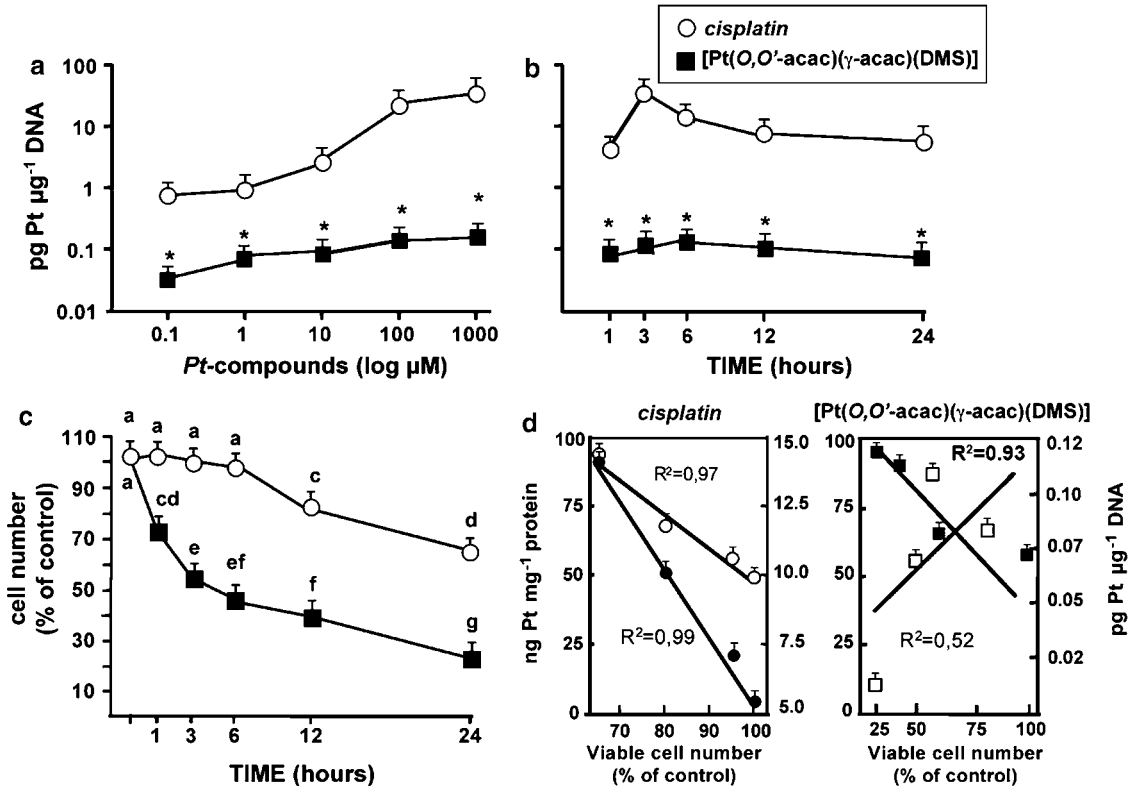

Figure 6 Relationship between the cytotoxicity of cisplatin and [Pt(*O,O'*-acac)(γ-acac)(DMS)] and the amount of the two compounds bound to proteins and DNA. (**a**) Cells were treated with or without increasing concentration of cisplatin or [Pt(*O,O'*-acac)(γ-acac)(DMS)]. (**b**) Cells were treated with or without 100 µM cisplatin or 10 µM [Pt(*O,O'*-acac)(γ-acac)(DMS)] for the indicated period. Platinum bound to DNA in MCF-7 was determined by atomic absorption spectrometry. Each point represents the means ± s.d. of three different experiments. Asterisks indicate values that are significantly different ($P<0.05$) from cisplatin at the same concentration and the same time point. (**c**) Cells were treated with or without 100 µM cisplatin or 10 µM [Pt(*O,O'*-acac)(γ-acac)(DMS)] for the indicated period. Viable cell number was determined by MTT assay, and the data are means ± s.d. of four different experiments, each with eight replicates, and are presented as % of control. Values with shared letters are not significantly different according to Bonferroni/Dunn *post hoc* tests. (**d**) Relationship between the cytotoxicity of cisplatin and [Pt(*O,O'*-acac)(γ-acac)(DMS)] and the amount of the two compounds bound to the DNA or present in the cell lysate. The previously obtained data were subjected to linear regression analysis; the data are the results of independent experiments presented as the means ± s.d.

inasmuch as JC-1-aggregate formation was abolished (Figure 10b).

The depolarizing agent carbonylcyanide-*m*-chloro-phenylhydrazone (5 µM), incubated for 10 min, was used as a positive control.

To examine the sequence of phenomena that link mitochondrial molecular events to cell death process, cytochrome *c* release, caspases activation and $\Delta\Psi_m$ were monitored simultaneously over several hours after apoptosis induction. MCF-7 cells were treated with 10 µM [Pt(*O,O'*-acac)(γ-acac)(DMS)], and cytosolic extracts were prepared at various times, under conditions that kept mitochondria intact. Cytosolic cytochrome *c* protein levels were measured by immunoblot analysis. Cytosol from untreated cells did not show detectable cytochrome *c* protein (Figure 10b). In contrast, cytosolic cytochrome *c* accumulated significantly after 15–60 min of treatment with [Pt(*O,O'*-acac)(γ-acac)(DMS)] (Figure 9a). At 60 min, cytochrome *c* was maximally released from mitochondria and no further increase was observed thereafter. The absence of porin in cytosolic extracts confirmed that our preparations were free of mitochondrial contamination (Figure 10b″).

Immunoblot analysis of the subcellular fractions showed that [Pt(*O,O'*-acac)(γ-acac)(DMS)] treatment led to the translocation of Bax protein to the mitochondria from the cytosol (Figure 10aa′) within 15–60 min. Translocation of Bax from the cytosolic compartment to the mitochondria has been shown to cooperate with Bid activation in the release of cytochrome *c* from mitochondria (Kroemer *et al.*, 1998). Hence, we investigated the localization of the truncated (activated) form of Bid (t-Bid) in MCF-7 cells treated with [Pt(*O,O'*-acac)(γ-acac)(DMS)] and observed the loss of t-Bid from the cytosol in response to [Pt(*O,O'*-acac)(γ-acac)(DMS)] treatment and its translocation to a mitochondria-containing fraction (Figure 10a). In addition, in mitochondrial fractions of [Pt(*O,O'*-acac)(γ-acac)(DMS)]-treated MCF-7 cells, Bax expression increased as the expression of an anti-apoptotic factor, Bcl-2, declined (Figure 10a). In the cytosol, cytochrome *c* binds apoptosis-activating factor-1, allowing recruitment of caspase-9 and formation of the apoptosome, resulting in caspase activation and execution of cell death (Kroemer *et al.*, 1998). The PARP cleavage product was detected slightly earlier than caspase-7 cleavage, at 30 min following exposure to [Pt(*O,O'*-acac)(γ-acac)(DMS)] as

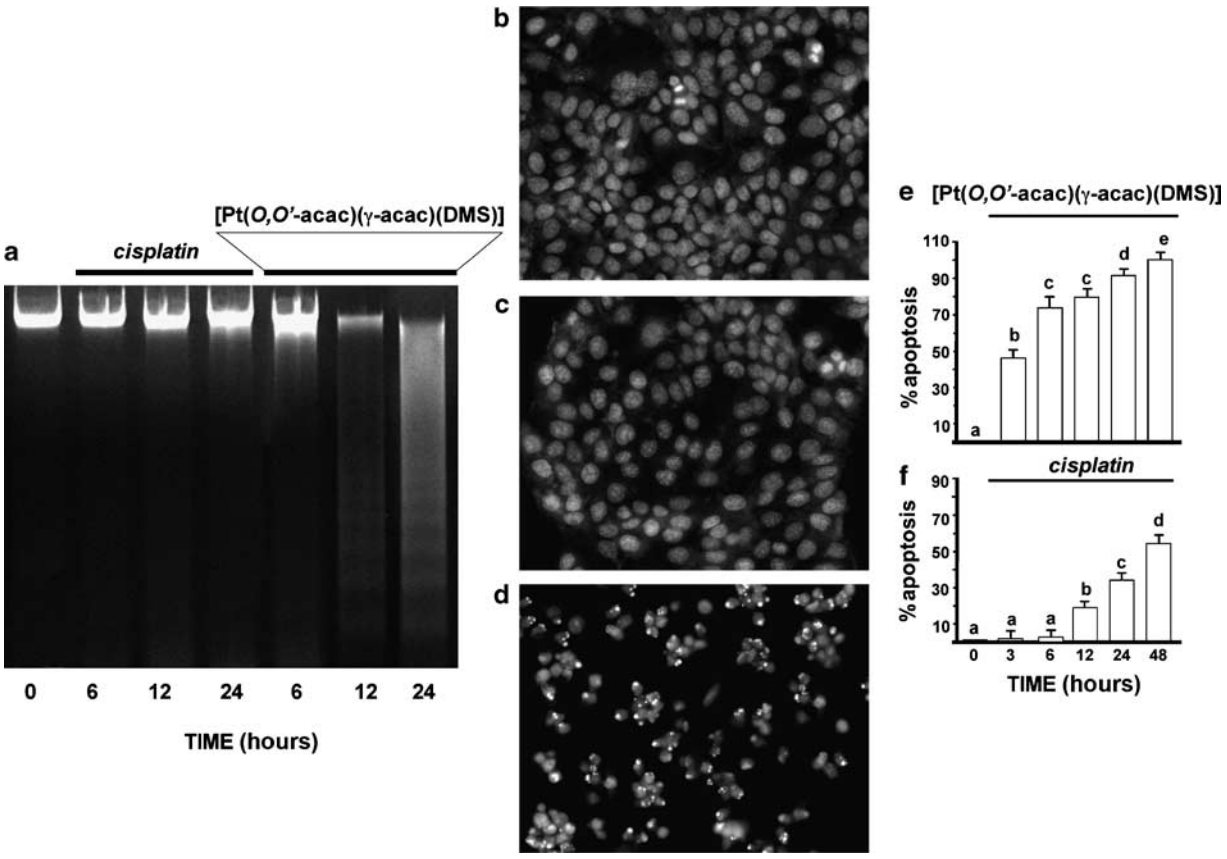

Figure 7 [Pt(*O,O*′-acac)(γ-acac)(DMS)]- and cisplatin-provoked apoptosis. (**a**) Visualization of DNA fragmentation in [Pt(*O,O*′-acac)(γ-acac)(DMS)]- and cisplatin-treated MCF-7 cells. Total DNA was isolated and separated on a 1% agarose gel. A representative example of three independent experiments is shown. (**b**–**d**) MCF-7 cells were treated or not (control, **b**) with cisplatin (**c**) and [Pt(*O,O*′-acac)(γ-acac)(DMS)] (**d**) for 6 h and then stained with DAPI; the representative fields of one of four independent experiments are shown (magnification × 400). (**e** and **f**) Quantification of the percentage of apoptotic nuclei obtained from cells stained with DAPI (means ± s.d.; $n = 4$), after treatment for different times with 10 μM [Pt(*O,O*′-acac)(γ-acac)(DMS)] or 100 μM cisplatin. Values with shared letters are not significantly different according to Bonferroni/Dunn *post hoc* tests.

quantified by densitometric scanning of the immunoblot (Figure 2b). In summary, these results show that cytochrome *c* release from mitochondria is an early event in the [Pt(*O,O*′-acac)(γ-acac)(DMS)]-induced apoptotic process in MCF-7 cells, occurring at the time of caspase-9- and before caspase-7-specific activation and preceding a decrease in $\Delta\Psi_m$.

Discussion

There is an increasing realization that chemotherapeutic agents act primarily by inducing cancer cell death through the mechanism of apoptosis (Clarke, 2003). However, there are many cancers that are intrinsically resistant to apoptosis, making it necessary to develop novel drugs for combination chemotherapy. Hence, we have synthesized a group of new platinum complexes for antitumour evaluation. These contained both an *O,O*′-chelated acetylacetonate and a sulphur ligand in the platinum coordination sphere (De Pascali *et al*., 2005; Muscella *et al*., 2007), which show low reactivity in a model reaction with purine bases monitored by ^{1}H NMR. All these platinum(II) compounds can induce cell death in the human cervical carcinoma HeLa cell line, with [Pt(*O,O*′-acac)(γ-acac)(DMS)] being the most effective (Muscella *et al*., 2007). Thus, it seemed appropriate to assess the ability of the [Pt(*O,O*′-acac)(γ-acac)(DMS)] complex to induce cell death in the relatively cisplatin-insensitive MCF-7 breast tumour cell line. The results we obtained provide evidence that [Pt(*O,O*′-acac)(γ-acac)(DMS)] may be a promising new anticancer agent, as it exhibited higher antitumour activity than cisplatin in *in vitro* tests on MCF-7 and other breast cancer cell lines differently expressing ERα/β (Figure 2 and Table 1). Among the cell lines used here, MCF-10A are the only ones considered to be normal, non-cancerous cells; MCF-10A appeared to be less sensitive to [Pt(*O,O*′-acac)(γ-acac)(DMS)] than MCF-7 cells in both the MTT and clonogenic assays (Figure 3 and Table 1). These preliminary data deserve further investigation, as it is important to determine whether [Pt(*O,O*′-acac)(γ-acac)(DMS)] is toxic specifically for cancer cells.

Consistent with the results from other studies (Janicke *et al*., 1998; Smith, 1999), we showed that MCF-7 cells are relatively insensitive to cisplatin, whereas [Pt(*O,O*′-acac)(γ-acac)(DMS)] efficiently induced apoptosis of these cells. Apoptosis induced by cisplatin is generally considered to be generated by the formation of covalent DNA adducts, which block replication and transcription, as well as reactive oxygen intermediates (Cepeda *et al*., 2007). However, the

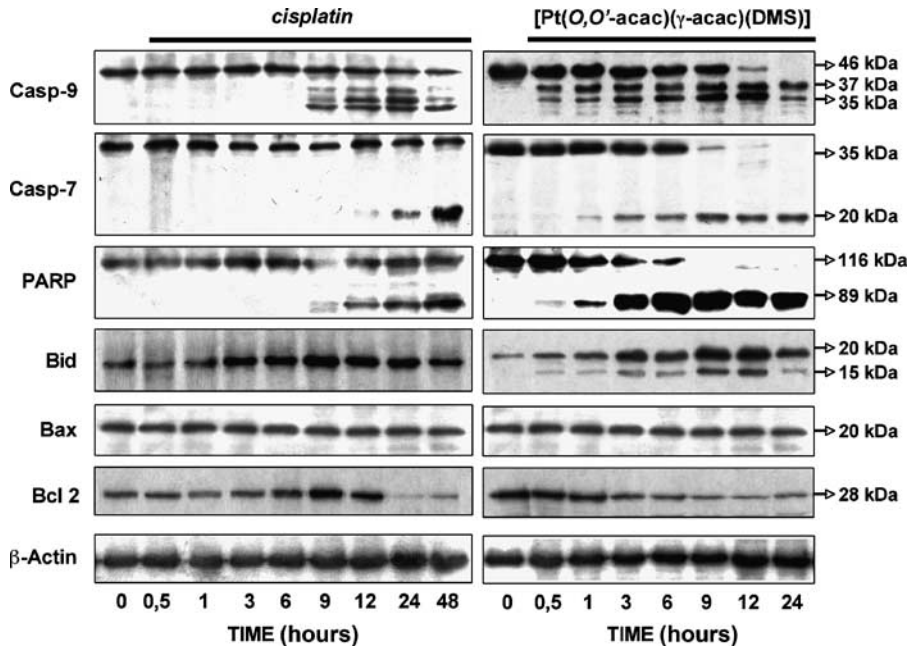

Figure 8 Effect of cisplatin and [Pt(*O,O*′-acac)(γ-acac)(DMS)] on the activation of caspase-7 and -9, the cleavage of PARP and on anti- and proapoptotic proteins. Cytosolic and nuclear proteins were obtained from MCF-7 cells, treated or not with 10 μM [Pt(*O,O*′-acac)(γ-acac)(DMS)] (right) or 100 μM cisplatin (left). Samples were dissolved in SDS sample buffer and separated on SDS gel. Immunoblotting was performed using monoclonal anti-PARP, anti-caspases-7 and -9, and Bid, Bax and Bcl2. Sequential incubation with anti-actin confirmed the equal protein loading. These results are representative of four independent experiments.

development of new platinum compounds was based on the hypothesis that compounds structurally dissimilar to cisplatin may have, by virtue of the formation of different types of platinum–DNA adducts, a spectrum of antitumour activity complementary to that of cisplatin. Interestingly, the reduced reactivity of the novel compound [Pt(*O,O*′-acac)(γ-acac)(DMS)] with purines (Figure 1) and DNA (Figure 6), observed in the present study, indicates that its cytotoxic activity may not necessarily require a reaction with DNA. On the other hand, the specific reactivity with sulphur ligands that allowed the synthesis of [Pt(*O,O*′-acac)(γ-acac)(DMS)], by selective substitution of the sulphoxide with the sulphide ligand, strongly suggests proteic thiols or thioether as the preferred target for these molecules. Indeed, as expected, *in vitro* substitution of sulphoxide with methionine lead to the almost instantaneous transformation of [Pt(*O,O*′-acac)(γ-acac)(DMS)] to [Pt(*O,O*′-acac)(γ-acac)(methionine)] (Figure 1). The reactivity of this compound could therefore be ascribed to its tendency to give sulphur ligand exchange at the platinum centre. It is noteworthy that DNA is also not the primary target of other metal complexes, such as the ruthenium imidazolium trans-imidazoledimethyl sulfoxide-tetrachlororuthenate (NAMI) and its analogue (ImH)*trans*-[Ru(Im)(Me_2SO)Cl_4] (NAMI-A) (Clarke, 2003) and the Au(I) complexes with 1,2-*bis*(diphenylphosphino)ethane, with 1,2-*bis*(dipyridylphosphino)ethane ligands (McKeage *et al*., 2002) and with monophosphine and diphosphine ligands (Caruso *et al*., 2003).

In accordance with what has been found for cisplatin (Gately and Howell, 1993), [Pt(*O,O*′-acac)(γ-acac)(DMS)] seemed to enter cells via a passive or facilitated passive transport, but it entered very quickly and its cellular accumulation was approximately 10 times higher than that of cisplatin (Figures 4b and c). This allowed us to use a 10-fold lower concentration of [Pt(*O,O*′-acac)(γ-acac)(DMS)] in further experiments. Despite this, the cytotoxic effects of 10 μM [Pt(*O,O*′-acac)(γ-acac)(DMS)] were stronger and faster than the those elicited by 100 μM cisplatin (Figure 6c). Another important difference was found in the cellular distribution of cisplatin and [Pt(*O,O*′-acac)(γ-acac)(DMS)]. While both gave approximately the same nuclei content, [Pt(*O,O*′-acac)(γ-acac)(DMS)] scarcely bound to DNA (approximately 100-fold lower than cisplatin, Figures 6a and b). Therefore, 10 μM [Pt(*O,O*′-acac)(γ-acac)(DMS)] was used for further studies, in which a more detailed analysis of cell death pathways was undertaken.

The proteolytic enzymes caspases have a critical role in the execution of apoptosis, and cisplatin may induce apoptosis through caspase-3-dependent and caspase-3-independent pathways (Henkels and Turchi, 1999). Although MCF-7 cells lack caspase-3 (Blanc *et al*., 2000), they undergo a caspase-mediated apoptosis when treated with [Pt(*O,O*′-acac)(γ-acac)(DMS)], as indicated by caspase-7, PARP cleavages and DNA fragmentation. Caspase-7 is highly related to caspase-3 and shows the same synthetic substrate specificity *in vitro* (Wei *et al*., 2000), suggesting that caspase-3 and -7 possibly have overlapping roles in apoptosis (Riedl *et al*., 2001). Without caspase-3, [Pt(*O,O*′-acac)(γ-acac)(DMS)]-treated MCF-7 cells may utilize an alternative caspase pathway to effect cell death (Riedl *et al*., 2001). Here, we demonstrated that caspase-7 was activated in [Pt(*O,O*′-acac)(γ-acac)(DMS)]-treated MCF-7 cells, that is, the 35-kDa proenzyme was cleaved into its active 17-kDa subunit. Synthesized as inactive precursors, caspases must be proteolytically cleaved

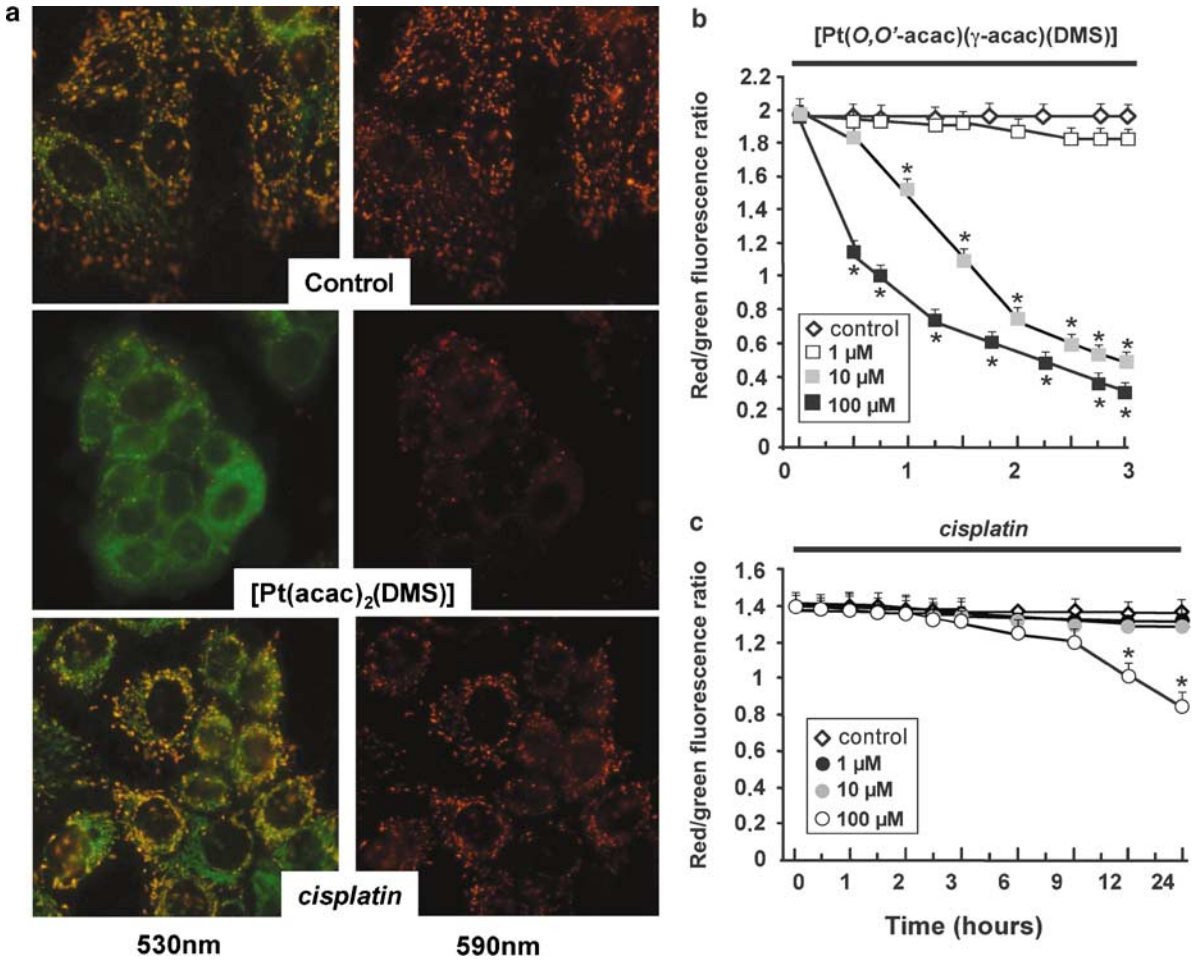

Figure 9 Effect of cisplatin and [Pt(*O,O*′-acac)(γ-acac)(DMS)] on $\Delta\Psi_m$ in MCF-7 cells. (**a**) Localization of JC-1 in MCF-7 cells, treated for 3 h or not with 10 μM [Pt(*O,O*′-acac)(γ-acac)(DMS)] or 100 μM cisplatin, by epifluorescence microscopy (right). Red fluorescence under green excitation corresponding to J-aggregates fluorescence (left). (**b**–**c**) Fluorescent spectra of JC-1 in MCF-7 cells treated or not with increasing concentrations of [Pt(*O,O*′-acac)(γ-acac)(DMS)] for indicated time (**b**) or treated or not with increasing concentrations of cisplatin for indicated time (**c**). The data are means ± s.d. of three different experiments and are presented as red J-aggregates/green monomer JC-1 fluorescence ratio. Asterisks indicate values that are significantly different ($P<0.05$) from cisplatin at the same concentration and the same time point.

to become active enzymes (Thornberry and Lazebnik, 1998). Overexpression of full-length caspase-7 in the MCF-7 cells does not induce apoptosis, whereas the activated 17-kDa subunit does induce apoptotic cell death (Duan *et al*., 1996). In both cisplatin- and [Pt(*O,O*′-acac)(γ-acac)(DMS)]-treated MCF-7 cells, the procaspase-9 activation occurred together with the generation of the mature form of caspase-7, indicating the involvement of the intrinsic pathway (Figure 8).

As regards the mitochondrial pathway, the most critical events during apoptosis are the release of cytochrome *c* from mitochondria into the cytoplasm, after the development of the mitochondrial transition pore. Cytochrome *c* in the cytoplasm complexes to and oligomerizes apoptosis-activating factor-1, leading to the activation of caspase-9 and the effector caspase cascade (Kroemer *et al*., 1998). The translocation of cytochrome *c* to cytoplasm generally occurs simultaneously with the decrease of $\Delta\Psi_m$ (Kroemer *et al*., 1998), another marker of subsequent cell death. Indeed, in [Pt(*O,O*′-acac)(γ-acac)(DMS)]-treated MCF-7 cells a significant decrease in $\Delta\Psi_m$ was already evident after 1 h and matched the release of mitochondrial cytochrome *c*, the activation of caspase-9, PARP cleavage and DNA fragmentation (Figure 10). While a decrease in $\Delta\Psi_m$ was observed earlier in [Pt(*O,O*′-acac)(γ-acac)(DMS)]-treated MCF-7 cells, in cisplatin-treated cells it occurred after caspase-9 activation (Figures 8 and 9), thus excluding the early involvement of the intrinsic pathway. At present, the precise connections linking [Pt(*O,O*′-acac)(γ-acac)(DMS)]-mediated apoptosis to the apoptotic death machinery are not known. However, it is clear that most, if not all, apoptotic stimuli from [Pt(*O,O*′-acac)(γ-acac)(DMS)] eventually funnel into the proapoptotic Bcl-2 proteins. Release of proapoptotic factors from mitochondria is controlled by Bcl-2 and Bax, members of the mitochondrial membrane-associated Bcl-2 family of proteins with opposing effects on cell life and death (Green and Reed, 1998). Overexpression of Bcl-2, an apoptotic inhibitor (Krajewski *et al*., 1993), has been shown to increase cisplatin resistance in a number of experimental models (Zangemeister-Wittke *et al*., 1998; Miyake *et al*., 1999; Mese *et al*., 2000). Bcl-2 overexpression in the mitochondrial outer membrane was associated with an upregulation of glutathione production,

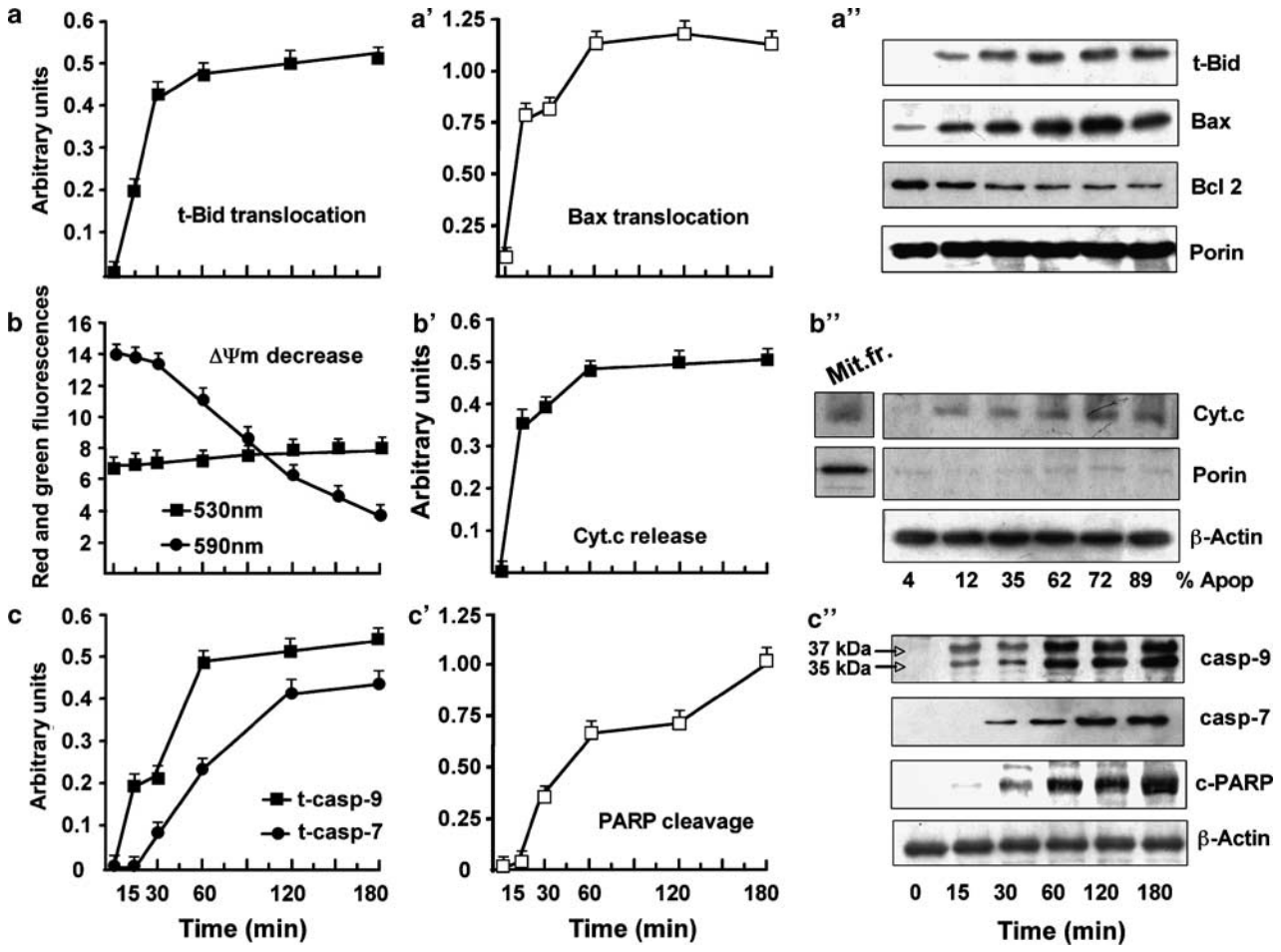

Figure 10 Mitochondrial cytochrome *c* enters the cytosol prior to activation of caspases and a complete reduction in $\Delta\Psi_m$ in MCF-7 cells treated with 10 μM [Pt(*O*,*O*′-acac)(γ-acac)(DMS)]. Mitochondrial fractions (Mit.fr.) were prepared at the indicated times of [Pt(*O*,*O*′-acac)(γ-acac)(DMS)] treatment, and the kinetics of t-Bid, Bax and Bcl-2 cytosol-to-mitochondria translocations were examined. t-Bid (**a**) and Bax (**a**′) translocations were quantified by densitometric scanning of the immunoblots obtained in Mit.fr. (**a**′′) and plotted against time after [Pt(*O*,*O*′-acac)(γ-acac)(DMS)] treatment. Fluorescences at 530 and 590 nm in cells loaded with JC-1 and treated with [Pt(*O*,*O*′-acac)(γ-acac)(DMS)]; mitochondrial transmembrane potential (ΔΨm) depolarization is estimated by a decrease in the red (590) to green (530) fluorescence ratio (**b**). (**b**′) Cytosolic extracts were prepared at the indicated times of [Pt(*O*,*O*′-acac)(γ-acac)(DMS)] and cytochrome *c* (Cyt.*c*), porin and actin were evaluated by immunoblot analysis (**b**′′). Porin served as an indicator for mitochondrial contamination of cytosolic extracts. Actin was used as a control for protein loading. The release of cytochrome *c* was quantified by densitometric scanning of the immunoblots and plotted against time (min) after [Pt(*O*,*O*′-acac)(γ-acac)(DMS)] treatment. The percentage of cells with low $\Delta\Psi_m$ is seen as a shift to weaker JC-1 fluorescence and was indicated at times after [Pt(*O*,*O*′-acac)(γ-acac)(DMS)] treatment. (**c**) Activation of procaspases-9 and -7 and cleavage of PARP were analysed by immunoblotting of cytosolic extracts. An arrow indicates the PARP cleavage product. The increases in caspases and PARP cleavage products were quantified by densitometric scanning of the immunoblots and the values were plotted against time after [Pt(*O*,*O*′-acac)(γ-acac)(DMS)] treatment. Results of densitometry analysis of immunoblots are means ± s.d. of three different experiments and the representative immunoblots are shown.

which contributes to MCF-7 cell survival by mechanisms independent of cisplatin inactivation or inhibition of DNA adduct formation (Rudin *et al*., 2003), and suppression of Bcl-2 expression reverses MCF-7 cell survival advantage (Basma *et al*., 2005). In contrast, Bax is a proapoptotic factor that translocates from the cytosol to the outer mitochondrial membrane where it can form heterodimers with Bcl-2 protein to form pores and mediate cytochrome *c* release. We found that [Pt(*O*,*O*′-acac)(γ-acac)(DMS)], but not cisplatin, apoptosis was associated with downregulation of Bcl-2 (Figure 8) and translocation of Bax into mitochondria from the cytosol. Our data also suggest that Bid is involved in [Pt(*O*,*O*′-acac)(γ-acac)(DMS)]-induced apoptosis. On induction of apoptosis, it has been demonstrated that Bid is cleaved and t-Bid translocates to mitochondria (Kroemer *et al*., 1998) to oligomerize and trigger the insertion of Bax (Eskes *et al*., 2000). It is important to note that apoptosis is not a prominent feature of DNA damage responses by cisplatin in this cell line (as in other epithelial cancer cell types) and cells may die by mechanisms other than apoptosis, such as autophagy (Levine, 2007). Bid expression increased markedly in breast cancer MCF-7 cells exposed to either [Pt(*O*,*O*′-acac)(γ-acac)(DMS)] or cisplatin, and during [Pt(*O*,*O*′-acac)(γ-acac)(DMS)]-mediated induction of apoptosis Bid was cleaved, t-Bid translocated to mitochondria fraction and $\Delta\Psi_m$ decreased. In contrast, no translocation or cleavage of Bid occurred in MCF-7 cells after cisplatin treatment. Our present data do not clarify how Bid is

activated. However, it is widely believed that activation of Bid requires its cleavage by caspase-8 or other proteases (Degli Esposti, 2002). Moreover, Bid is also able to oligomerize and trigger the insertion of Bax in isolated mitochondria by excitotoxic injury (Eskes *et al*., 2000), and subsequent changes in phospholipid composition may convert Bid into a t-Bid that is subsequently able to activate Bax and mitochondrial cell death pathways. In addition, a kinase-mediated regulation of Bid activation has also been suggested (Degli Esposti, 2002).

The results from the present study show that the mechanism for apoptosis is functional in MCF-7 cells and [Pt(*O,O*′-acac)(γ-acac)(DMS)] is able to activate the mitochondrial pathway. This is particularly important since tumours accumulate mutations that increase their resistance to apoptotic inducers, for example, attenuation of caspase-3 has been associated with multidrug acquired resistance (Kojima *et al*., 1998). Thus, finding new therapeutic agents that induce caspase-3-independent apoptosis may have valuable clinical implications. From this viewpoint, [Pt(*O,O*′-acac)(γ-acac)(DMS)] may evoke an apoptotic pathway different from that of clinical oncology drugs such as doxorubicin and etoposide (Yang *et al*., 2001). Finally, the possibility that [Pt(*O,O*′-acac)(γ-acac)(DMS)] targets mitochondrial permeability provides us with new opportunities for therapeutic intervention and may help to overcome resistance to standard cancer therapies (Makin and Dive, 2001).

Acknowledgements

We are grateful to the Italian MIUR for project grant support (PRIN 2004-prot. 2004050714).

Conflict of interest

The authors state no conflict of interest.

References

Basma H, El-Refaey H, Sgagias MK, Cowan KH, Luo X, Cheng PW (2005). BCL-2 antisense and cisplatin combination treatment of MCF-7 breast cancer cells with or without functional p53. *J Biomed Sci* **12**: 999–1011.

Blanc C, Deveraux QL, Krajewski S, Janicke RU, Porter AG, Reed JC *et al.* (2000). Caspase-3 is essential for procaspase-9 processing and cisplatin-induced apoptosis of MCF-7 breast cancer cells. *Cancer Res* **60**: 4385–4390.

Boatright KM, Salvesen GS (2003). Mechanisms of caspase activation. *Curr Opin Cell Biol* **15**: 725–731; Review.

Caruso F, Rossi M, Tanski J, Pettinari C, Marchetti F (2003). Antitumor activity of the mixed phosphine gold species chlorotriphenylphosphine-1,3-*bis*(diphenylphosphino)propanegold(I). *J Med Chem* **46**: 1737–1742.

Cepeda V, Fuertes MA, Castilla J, Alonso C, Quevedo C, Perez JM (2007). Biochemical mechanisms of cisplatin cytotoxicity. *Anticancer Agents Med Chem* **7**: 3–18; Review.

Clarke MJ (2003). Ruthenium metallopharmaceuticals. *Coord Chem Rev* **236**: 209–233.

De Pascali SA, Papadia P, Ciccarese A, Pacifico C, Fanizzi FP (2005). First examples of β-diketonate platinum(II) complexes with sulfoxide ligands. *Eur J Inorg Chem* **5**: 788–796.

Degli Esposti M (2002). The roles of Bid. *Apoptosis* **7**: 433–440.

Duan H, Chinnaiyan AM, Hudson PL, Wing JP, He W-W, Dixit VM (1996). CE-LAP3, a novel mammalian homologue of the *Caenorhabditis elegans* cell death protein Ced-3 is activated during Fas- and tumor necrosis factor-induced apoptosis. *J Biol Chem* **271**: 1621–1625.

Eskes R, Desagher S, Antonsson B, Martinou JC (2000). Bid induces the oligomerization and insertion of Bax into the outer mitochondrial membrane. *Mol Cell Biol* **20**: 929–935.

Filardo EJ, Quinn JA, Bland KI, Frackelton Jr AR (2000). Estrogen-induced activation of Erk-1 and Erk-2 requires the G protein-coupled receptor homolog, GPR30, and occurs via *trans*-activation of the epidermal growth factor receptor through release of HB-EGF. *Mol Endocrinol* **14**: 1649–1660.

Gately DP, Howell SB (1993). Cellular accumulation of the anticancer agent cisplatin: a review. *Br J Cancer* **67**: 1171–1176.

Girdler F, Browell DA, Cunliffe WJ, Shenton BK, Hemming JD, Scorer P *et al.* (2001). Use of the monoclonal antibody DAKO-ERbeta (8D5-1) to measure oestrogen receptor beta in breast cancer cells. *Cytometry* **45**: 65–72.

Green DR, Reed JC (1998). Mitochondria and apoptosis. *Science* **281**: 1309–1312; Review.

Henkels KM, Turchi JJ (1999). Cisplatin-induced apoptosis proceeds by caspase-3-dependent and -independent pathways in cisplatin-resistant and -sensitive human ovarian cancer cell lines. *Cancer Res* **59**: 3077–3083.

Hu YF, Lau KM, Ho SM, Russo J (1998). Increased expression of estrogen receptor beta in chemically transformed human breast epithelial cells. *Int J Oncol* **12**: 1225–1228.

Isaac N, Panzarella T, Lau A, Mayers C, Kirkbride P, Tannock IF *et al.* (2002). Concurrent cyclophosphamide, methotrexate, and 5-fluorouracil chemotherapy and radiotherapy for breast carcinoma: a well tolerated adjuvant regimen. *Cancer* **95**: 696–703.

Janicke RU, Sprengart ML, Wati MR, Porter AG (1998). Caspase-3 is required for DNA fragmentation and morphological changes associated with apoptosis. *J Biol Chem* **273**: 9357–9360.

Kaufmann SH, Desnoyers S, Ottaviano Y, Davidson NE, Poirier GG (1993). Specific proteolytic cleavage of poly(ADP-ribose) polymerase: an early marker of chemotherapy-induced apoptosis. *Cancer Res* **53**: 3976–3985.

Kojima H, Endo K, Moriyama H, Tanaka Y, Alnemri ES, Slapak CA *et al.* (1998). Abrogation of mitochondrial cytochrome *c* release and caspase-3 activation in acquired multidrug resistance. *J Biol Chem* **273**: 16647–16650.

Krajewski S, Tanaka S, Takayama S, Schibler MJ, Fenton W, Reed JC (1993). Investigation of the subcellular distribution of the bcl-2 oncoprotein: residence in the nuclear envelope, endoplasmic reticulum, and outer mitochondrial membranes. *Cancer Res* **53**: 4701–4714.

Kroemer G, Dallaporta B, Resche-Rigon M (1998). The mitochondrial death/life regulator in apoptosis and necrosis. *Annu Rev Physiol* **60**: 619–642; Review.

Levine B (2007). Cell biology: autophagy and cancer. *Nature* **446**: 745–747.

Makin G, Dive C (2001). Modulating sensitivity to drug-induced apoptosis: the future for chemotherapy? *Breast Cancer Res* **3**: 150–153.

McKeage MJ, Maharaj L, Berners-Price SJ (2002). Mechanisms of cytotoxicity and antitumor activity of gold(I) phosphine complexes: the possible role of mitochondria. *Coord Chem Rev* **232**: 127–135.

Mese H, Sasaki A, Alcalde RE, Nakayama S, Matsumura T (2000). Regulation of apoptosis reduction in the cisplatin-resistant A431 cell line by Bcl-2 and CPP32. *Chemotherapy* **46**: 69–76.

Miyake H, Hara I, Yamanaka K, Arakawa S, Kamidono S (1999). Synergistic enhancement of resistance to cisplatin in human bladder cancer cells by over expression of mutant-type p53 and Bcl-2. *J Urol* **162**: 2176–2181.

Muscella A, Calabriso N, De Pascali SA, Urso L, Ciccarese A, Fanizzi FP *et al.* (2007). New platinum(II) complexes containing both an *O,O*′-chelated acetylacetonate ligand and a sulfur ligand in the

platinum coordination sphere induce apoptosis in HeLa cervical carcinoma cells. *Biochem Pharmacol* **74**: 28–40.

Muscella A, Greco S, Elia MG, Storelli C, Marsigliante S (2002). Angiotensin II stimulation of Na^+/K^+ATPase activity and cell growth by calcium-independent pathway in MCF-7 breast cancer cells. *J Endocrinol* **173**: 315–323.

Perillo B, Sasso A, Abbondanza C, Palumbo G (2000). 17-*h*-estradiol inhibits apoptosis in MCF-7 cells, inducing Bcl-2 expression via two estrogen-responsive elements present in the coding sequence. *Mol Cell Biol* **8**: 2890–2901.

Riedl SJ, Fuentes-Prior P, Renatus M, Kairies N, Krapp S, Huber R *et al*. (2001). Structural basis for the activation of human procaspase-7. *Proc Natl Acad Sci USA* **98**: 790–795.

Rudin CM, Yang Z, Schumaker LM, VanderWeele DJ, Newkirk K, Egorin MJ *et al*. (2003). Inhibition of glutathione synthesis reverses Bcl-2-mediated cisplatin resistance. *Cancer Res* **63**: 312–318.

Skehan P, Storeng R, Scudiero D, Monks A, McMahon J, Vistica D *et al*. (1990). New colorimetric cytotoxicity assay for anticancer-drug screening. *J Natl Cancer Inst* **82**: 1107–1112.

Smiley ST, Reers M, Mottola-Hartshorn C, Lin M, Chen A, Smith TW *et al*. (1991). Intracellular heterogeneity in mitochondrial membrane potentials revealed by a J-aggregate-forming lipophilic cation JC-1. *Proc Natl Acad Sci USA* **88**: 3671–3675.

Smith ML (1999). Mdm2 sensitizes MCF7 breast cancer cells to cisplatin or carboplatin. *Breast Cancer Res Treat* **58**: 99–105.

Thornberry NA, Lazebnik Y (1998). Caspases: enemies within. *Science* **281**: 1312–1316.

Wei Y, Fox T, Chambers SP, Sintchak J, Coll JT, Golec JM *et al*. (2000). The structures of caspases-1, -3, -7 and -8 reveal the basis for substrate and inhibitor selectivity. *Chem Biol* **7**: 423–432.

Xu C, Meikrantz W, Schlegel R, Sager R (1995). The human papilloma virus 16E6 gene sensitizes human mammary epithelial cells to apoptosis induced by DNA damage. *Proc Natl Acad Sci USA* **92**: 7829–7833.

Yang XH, Sladek TL, Liu X, Butler BR, Froelich CJ, Thor AD (2001). Reconstitution of caspase-3 sensitizes MCF-7 breast cancer cells to doxorubicin- and etoposide-induced apoptosis. *Cancer Res* **61**: 348–354.

Zangemeister-Wittke U, Schenker T, Luedke GH, Stahel RA (1998). Synergistic cytotoxicity of bcl-2 antisense oligodeoxynucleotides and etoposide, doxorubicin and cisplatin on small-cell lung cancer cell lines. *Br J Cancer* **78**: 1035–1042.